

# Microcapsules for Enhanced Cargo Retention and Diversity

Maximilian A. Zieringer, Nick J. Carroll, Alireza Abbaspourrad, Stephan A. Koehler, and David A. Weitz\*

**P**revention of undesired leakage of encapsulated materials prior to triggered release presents a technological challenge for the practical application of microcapsule technologies in agriculture, drug delivery, and cosmetics. A microfluidic approach is reported to fabricate perfluoropolyether (PFPE)-based microcapsules with a high core-shell ratio that show enhanced retention of encapsulated actives. For the PFPE capsules, less than 2% leakage of encapsulated model compounds, including Allura Red and  $\text{CaCl}_2$ , over a four week trial period is observed. In addition, PFPE capsules allow cargo diversity by the fabrication of capsules with either a water-in-oil emulsion or an organic solvent as core. Capsules with a toluene-based core begin a sustained release of hydrophobic model encapsulants immediately upon immersion in an organic continuous phase. The major contribution on the release kinetics stems from the toluene in the core. Furthermore, degradable silica particles are incorporated to confer porosity and functionality to the otherwise chemically inert PFPE-based polymer shell. These results demonstrate the capability of PFPE capsules with large core-shell ratios to retain diverse sets of cargo for extended periods and make them valuable for controlled release applications that require a low residual footprint of the shell material.

## 1. Introduction

The utility of microcapsules for effective cargo storage and targeted release is of considerable importance in agriculture, self-healing materials, drug delivery, and cosmetics.<sup>[1–3]</sup> Ideal polymeric microcapsules should be composed of a membrane that efficiently captures and retains actives until their release is triggered. Although a variety of sophisticated capsule materials capable of responding to an external trigger have been

developed, leakage of actives is typically observed; this drawback presents a technological challenge for the practical application of capsule technologies.<sup>[4]</sup> Unwanted cargo loss from microcapsules prior to triggering results from the shell material's inherent permeability to encapsulated molecules. Capsule shells fabricated from linear hydrophobic polymers, such as glyceride wax, paraffin, or poly(lactic acid) derivatives, form a nonhomogeneous structure during solidification; this leads to the undesired formation of small defects and consequently, to loss of encapsulated actives.<sup>[5]</sup> This limitation can be mitigated by fabrication of thick shell structures; however, this approach results in small core-shell ratios and a large residual footprint after triggered release of encapsulated actives.<sup>[6]</sup> These drawbacks may diminish or compromise the use of microcapsule technologies for certain applications. Homogeneous, defect-free shell structures can be achieved by covalent crosslinking of monomers or macromonomers. The resultant dense polymeric networks have reduced mesh size making them an attractive alternative to shells composed

Dr. M. A. Zieringer, Dr. N. J. Carroll, Dr. A. Abbaspourrad,  
Dr. S. A. Koehler, Prof. D. A. Weitz  
School of Engineering and Applied Sciences  
and Department of Physics  
Harvard University  
Cambridge, MA 02138, USA  
E-mail: weitz@seas.harvard.edu



DOI: 10.1002/smll.201403175

of linear polymeric building blocks.<sup>[7]</sup> However, the monomers used for membrane fabrication are either hydrophilic or lipophilic; this limits both cargo diversity and fluid combinations which can be used.

Leakage prior to triggering may also result from the microcapsule fabrication process. Conventional encapsulation techniques, such as bulk emulsification, spray drying, or interfacial polymerization produce microcapsules with a wide range of sizes, shell thicknesses, and structures, and thus offer poor control of their release properties.<sup>[8,9]</sup> In contrast to these techniques, microfluidic encapsulation allows the production of monodisperse capsules with high encapsulation efficiency.<sup>[10]</sup> Furthermore, microfluidic technologies offer a route to precisely control the payload and the core-shell ratio of microcapsules. Thus, the utility of microcapsules could potentially be extended by combining microfluidic techniques with shell materials capable of preventing leakage for a wide and diverse range of cargo.

A promising route to achieve capsules with these unique properties is the use of crosslinkable perfluorinated monomers. Perfluoropolyethers (PFPE) are composed of repeat units of small perfluorinated aliphatic oxides and have remarkable properties including low surface tension, excellent spreading, high fluidity, and antifriction.<sup>[11–13]</sup> They are thermally and chemically stable as well as biologically inert.<sup>[14]</sup> Furthermore, perfluoropolyethers are concurrently hydrophobic and lipophobic which potentially enables the encapsulation of both hydrophilic and hydrophobic cargos. However, fabrication of microcapsules using crosslinkable PFPE macromonomers has not yet been demonstrated; thus, there remains an unmet need for fabrication of low-leakage microcapsules that are compatible with a wide variety of core solvents.

In this paper, we describe a microfluidic approach for fabricating PFPE-based microcapsules that show enhanced retention of encapsulated model compounds in addition to cargo diversity. We form water–fluorinated–water (W/F/W) template double emulsion droplets to encapsulate hydrophilic compounds within a PFPE dimethacrylate middle layer in a combined coflow and flow-focusing microfluidic device. To obtain PFPE capsules, we consolidate the middle layer of the template double emulsion drops using an in situ photopolymerization method. The perfluorinated segments of the macromonomers limit the swelling of the resulting polymer network in both aqueous and organic solvents, resulting in a highly effective diffusion barrier for the encapsulated cargo. This barrier allows the fabrication of microcapsules with a large core to shell ratio and consequently, high payload per capsule. We demonstrate retention of a water-soluble molecular dye within the resultant microcapsules over a trial period of four weeks. In addition, these capsules can retain cargo as small as ions for the same period in the absence of osmotic stress. The inherent hydro- and lipophobicity of the PFPE segments allow fabrication of

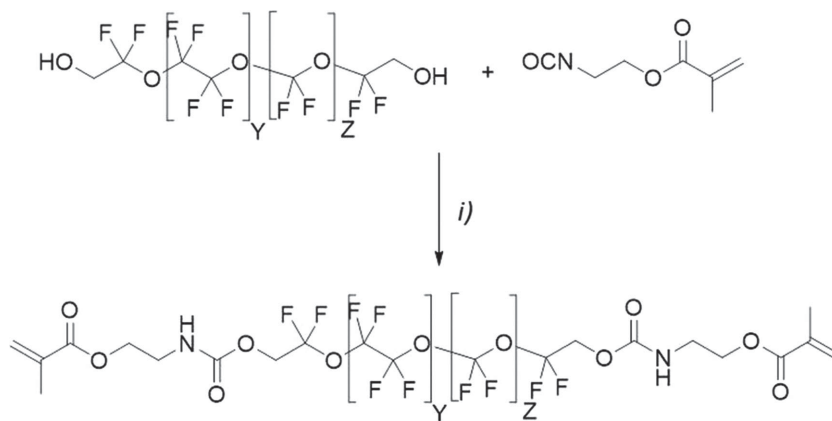
microcapsules with unprecedented cargo diversity; we demonstrate this capability by encapsulating organic liquid and a water-in-oil emulsion. We thus demonstrate effective encapsulation of a diverse set of cores, including aqueous, organic, and emulsion liquids. Our investigation focuses on the synergistic effect of crosslinking low surface energy polymers for effective retention of molecular cargo. PFPE microcapsules have great future potential for practical utility for long-term encapsulation of actives common to many applications such as drug delivery, self-healing materials, cosmetics, and within the automotive industry.

## 2. Results and Discussion

### 2.1. Microfluidic Fabrication of PFPE Microcapsules with Aqueous and Organic Cores

For the precursor of an inert shell, we select a commercially available PFPE diol, (poly(tetrafluoroethylene oxide-co-difluoromethylene oxide)  $\alpha,\omega$ -diol, and catalytically attach methacrylate moieties to the terminal hydroxyl groups, as shown in **Scheme 1**. The PFPE block confers chemical inertness as well as hydro- and lipophobicity to the resultant capsule membrane. The methacrylate groups facilitate photopolymerization of the PFPE monomers to produce a highly crosslinked homogeneous polymeric network. The resulting polymer displays a contact angle of 102° with water and a contact angle of 75° with hydrocarbon solutions, such as mineral oil. These contact-angle measurements indicate that despite the presence of its polar carboxyl and carbamate moieties the polymer retains teflon-like physicochemical properties.

To produce PFPE microcapsules, we form W/F/W double emulsion drops as templates using a glass-capillary microfluidic device that combines coflow and flow-focusing geometries.<sup>[15]</sup> The device consists of two opposing round glass capillaries within a square glass tube, as shown in **Figure 1a,b**. The inner fluid is an aqueous solution of the encapsulant which is injected through the tapered end of one round capillary into the collection capillary. To form a coaxial flow, we inject the middle fluid, PFPE dimethacrylate



**Scheme 1.** Synthesis of PFPE shell precursor. i) Dibutyltin diacetate (cat.), 60:40 Novec 7100:THF, 50 °C, 24 h, Ar.

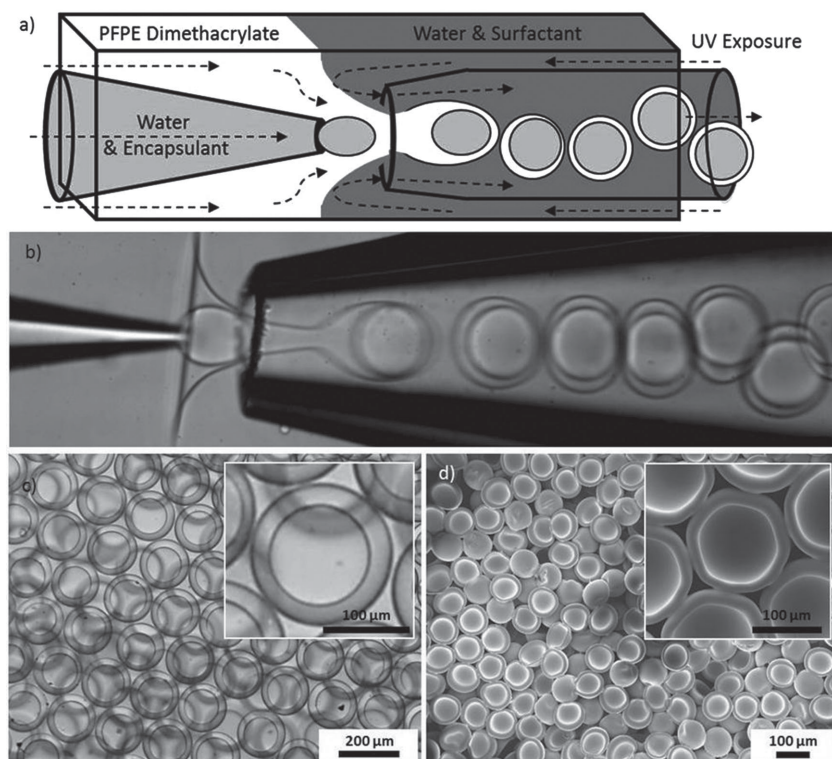


**Figure 1.** a) Schematic of combined coflow and flow-focusing glass-capillary device. b) Double emulsion templates for PFPE capsules formed in capillary microfluidic device. c) Optical and d) SEM images of resultant PFPE capsules; scale bars: 100 μm.

and a radical initiator, 2,2-dimethoxy-2-phenylacetophenone, through the outer capillary in the same direction as the inner fluid. The outermost fluid is water-containing surfactant, 10 wt% polyvinyl alcohol, and is injected through the outer capillary from the opposite direction, hydrodynamically flow-focusing the coaxial stream. Monodisperse double emulsion drops, consisting of an inner water droplet surrounded by the PFPE dimethacrylate middle phase, are formed at the orifice of the collection capillary. The microfluidic device provides exquisite control over the fabrication of the emulsion, producing a continuous stream of double emulsion drops which are monodisperse and have a well-defined core shell ratio, as shown in Figure 1b. Immediately after drop formation, we in situ photopolymerize the PFPE dimethacrylate to minimize the effects of gravitational settling due to the density mismatch of the inner and middle phases, thereby forming spatially homogeneous shells. Since the middle phase contains no solvent, no additional evaporation step is required enabling us to directly and independently adjust the shell thickness from the flow rates. Optical microscope and SEM images of the resultant capsules are shown in Figure 1c,d, respectively.

In addition to aqueous cargo, PFPE capsules allow the encapsulation of a wide variety of organic solvents using our microfluidic approach without further modification. To demonstrate cargo diversity for both organic and inhomogeneous fluids, we encapsulate a preformed water-in-oil (W/O) emulsion of water drops containing FITC dye dispersed in hexadecane. We employ the same device geometry to form monodisperse double emulsion drops in which the inner phase consists of the W/O emulsion, as shown in Figure 2. As indicated by the contact angles of water and mineral oil, the PFPE shell material is simultaneously hydro- and lipophobic and therefore, is orthogonal to both the aqueous and the oil phases of the encapsulated emulsion. Such diversity further enhances the promise of PFPE-derived capsules for versatile and practical applications.

## 2.2. Retention of Aqueous Cargo

We quantify the leakage of encapsulants prior to release using 1 wt% aqueous solution of Allura Red as the encapsulant. The nontoxic Allura Red serves as model compound to mimic the diffusion behavior of water-soluble cargo molecules in the molecular weight range around 500 g mol<sup>-1</sup> and was previously used to investigate microcapsule encapsulation.<sup>[6]</sup> We fabricate PFPE microcapsules with a core-shell ratio of

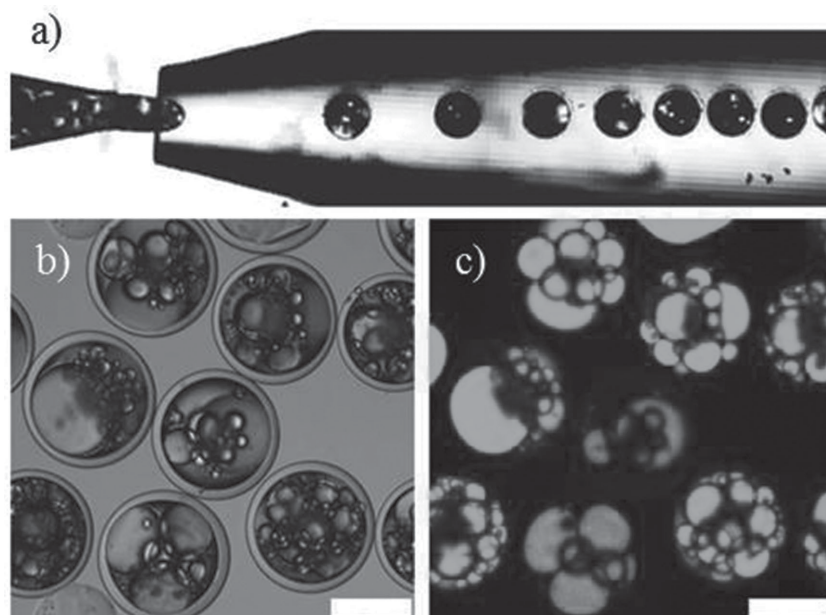


**Figure 2.** a) Double emulsion templates for PFPE capsules with emulsion cores formed in capillary microfluidic device. b) Optical image of PFPE microcapsules loaded with an emulsion of water in hexadecane. c) Confocal image of fluorescein water droplets of the encapsulated emulsion; scale bar = 100 μm.



1/0.8 v/v and monitor the release of dye into the continuous phase. To ensure an even distribution of released dye throughout the supernatant, we vortex the sealed vial containing the microcapsules prior to each measurement. After four weeks, only 1% of the encapsulated dye has leaked into the continuous phase, as shown qualitatively in the photographs of **Figure 3a** and quantitatively via UV/vis spectroscopy measurements in **Figure 3b** (blue diamonds). A previous encapsulation and release investigation on nonporous thin-shell crosslinked silicone-based capsules reveal complete leakage of a similar MW hydrophilic dye, fluorescein, on time frames of about seven days.<sup>[16]</sup> This hints at the importance of the synergistic effect of both crosslinking and intrinsic hydrophobicity of the membrane material on enhanced long term encapsulation of hydrophilic molecular cargo. Next, to evaluate capsule retention of ions, we encapsulate an aqueous 1.8 M  $\text{CaCl}_2$  solution and measure the change in conductivity of the outer fluid over time. Dissociated ions are considerably smaller than organic dyes such as Allura Red and, typically, can even penetrate solidified capsule shells.<sup>[17]</sup> To counteract the osmotic imbalance of the ions, we add nonconductive glucose to the outer fluid. Over a four week trial period only 2% of the encapsulated ions are lost as shown in **Figure 3b** (red circles). In contrast, if the osmotic pressure is not balanced by using pure deionized (DI) water as outer

fluid, we observe a greater rate of cargo loss, as illustrated by the black triangles in **Figure 3b**. There is an increase in the diffusion of ions through the shell during the first two weeks when compared to the case of nonstressed capsules. Osmotic stress modifies the activation barrier for diffusion, resulting in enhanced loss of cargo.<sup>[17]</sup> After two weeks, we observe a sharp increase in shell permeability which is not attributable to passive diffusion. As shown in the inset of **Figure 3b**, inspection of the capsules after the four week period reveals a bimodal population within the sample: capsules with diameters approximately twice their initial size, and a smaller subset of capsules which have burst due to the applied osmotic stress. As is the case for organic-based acrylic membranes,<sup>[18,19]</sup> water is also permeable to the PFPE-derived membranes under osmotic stress. Thus, the sharp increase in released ions is due to the fraction of capsules which begin bursting and releasing their cargo following two weeks of incubation and represents a simple release mechanism.

### 2.3. Retention of Organic Cargo

To examine the impact of organic solvents on cargo retention, we fabricate PFPE capsules that contain an  $8 \times 10^{-3}$  M solution of a model organic active, Nile Red, in toluene with a core-shell ratio of 1/0.2 v/v, as illustrated in **Figure 4a**. We split

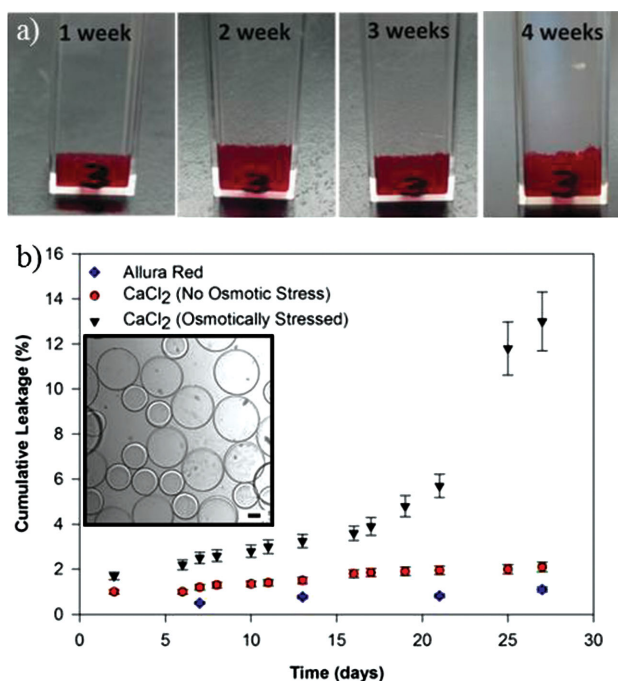


**Figure 3.** a) Photographs of Allura Red-loaded capsules suspended in water over four week period. The number of capsules remains constant during the trial period. The apparent variation in capsule volume within the sealed vials is due to rearrangement caused by vortexing. b) Graph showing the leakage of encapsulated model compounds. Percentage of Allura Red leaked over four weeks (blue diamonds). Percentage of  $\text{CaCl}_2$  ions leaked as a function of time for capsules under osmotic stress (black triangles) and capsules under no imposed osmotic tensile stress (red circles). Inset: Optical image of mixed population of microcapsules either under osmotic stress (large capsules) or ruptured (small capsules) at  $t = 25$  days; scale bar = 100  $\mu\text{m}$ .

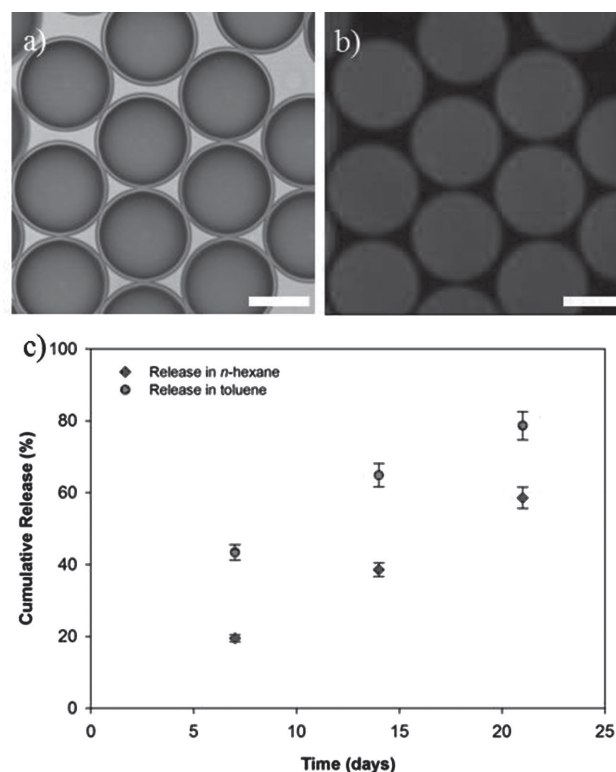


**Figure 4.** a) Optical image of PFPE microcapsules loaded with a solution of Nile Red in toluene. b) Confocal image of the Nile Red in the core; scale bars = 100  $\mu\text{m}$ . c) Graph showing cumulative release of low MW hydrophobic cargo molecules over three weeks. Percentage of Nile Red released in toluene (red triangles). Percentage of Nile Red released in hexane (blue squares).

the capsules into two batches, decant the supernatant, and then wash with DI water to remove the surfactant. Next, we suspend and incubate the first batch in hexane and the second batch in toluene; we monitor the cumulative release of Nile Red into the supernatant over the course of 21 days using UV/vis spectroscopy. Our results indicate a strong dependence of the release kinetics on the exterior solution employed. In contrast to their behavior in water, these capsules begin a sustained release of Nile Red immediately upon exposure to an organic continuous phase; the capsules lose 59% and 80% of the encapsulated Nile Red in hexane and toluene, respectively, as shown in Figure 4b (blue squares and red triangles).

To determine the permeability coefficients of the capsule shells, we use Fick's law in the limit of low concentrations and low shell permeability<sup>[17]</sup> for fitting the fractional release of dye to

$$X(t) = 1 - \exp\left(-\frac{3P}{a}t\right) \quad (1)$$

Here,  $X(t)$  is the fractional release of dye,  $a$  is the capsule radius, and  $P$  is the permeability coefficient. Capsules dispersed in toluene have twice the permeability of those dispersed in hexane, the permeability coefficients are  $2.2 \times 10^{-9}$  and  $1.1 \times 10^{-9} \text{ cm s}^{-1}$ , respectively. This twofold increase reveals the contribution of the outer fluid to the observed release kinetics and is expected since the swelling of PFPE membranes in hexane is negligible.<sup>[14]</sup> A significant contribution to the sustained release of encapsulated dye can be attributed to the inner carrier fluid. By  $^1\text{H-NMR}$  measurements we determine that toluene has a solubility of about 10 wt% in the PFPE dimethacrylate; solubility parameters are indicators for potential swelling by the solvent on a resultant polymer.<sup>[20]</sup> Swelling of the shell network leads to a lower diffusion barrier, and therefore to an accelerated leakage of encapsulated Nile Red.<sup>[21]</sup> Implementation of an appropriate carrier solvent into the capsule formulation provides a simple method to control the diffusivity and therefore, the release kinetics.

#### 2.4. Introduction of Porosity to the PFPE Matrix

A promising approach to confer additional functionality to crosslinked capsule shells without compromising their physicochemical properties is the incorporation of colloids into the matrix.<sup>[22,23]</sup> For an example, we produce porous PFPE shells by using colloidal templating as a porogen-based approach. We incorporate degradable micrometer-sized silica particles that have been derivatized with a surface coupling agent to confer hydrophobicity for dispersion into the PFPE dimethacrylate

matrix. Surface functionalization of silica particles with aliphatic silanes leads to instant precipitation of the silica particles from the monomer; therefore, we coat silica with a fluorinated silane, (heptadecafluoro 1,1,2,2-tetrahydrodecyl) trichlorosilane, to form a reasonably dispersed silica colloidal suspension within the monomer, as shown in Figure 5a. Upon formation of microcapsules using our microfluidic strategy, we observe silica particles protruding at the capsule surface as demonstrated in Figure 5b. We observe minor aggregation of the silica particles during shell solidification which indicates some colloidal instability during monomer polymerization. Upon exposure to an alkaline continuous fluid of pH = 10, the silica dissolves, resulting in micrometer-sized voids within the capsule shell, as observed in Figure 5c,d.

### 3. Conclusion

We use microfluidics to fabricate thin-shell PFPE capsules that show excellent retention of encapsulated actives. Moreover, our shell material allows for the encapsulation of aqueous as well as organic cargo through its inherent hydro- and lipophobicity. We produce these PFPE microcapsules using double emulsion drops as templates; our microfluidic approach provides a versatile way to produce capsules with a wide variety of aqueous, organic, and even multiphase cargo without further device or shell material modification. The resulting PFPE capsules retain aqueous cargo without noticeable leakage; for example, over 98% of encapsulated  $\text{CaCl}_2$  is retained within the capsules over a course of four

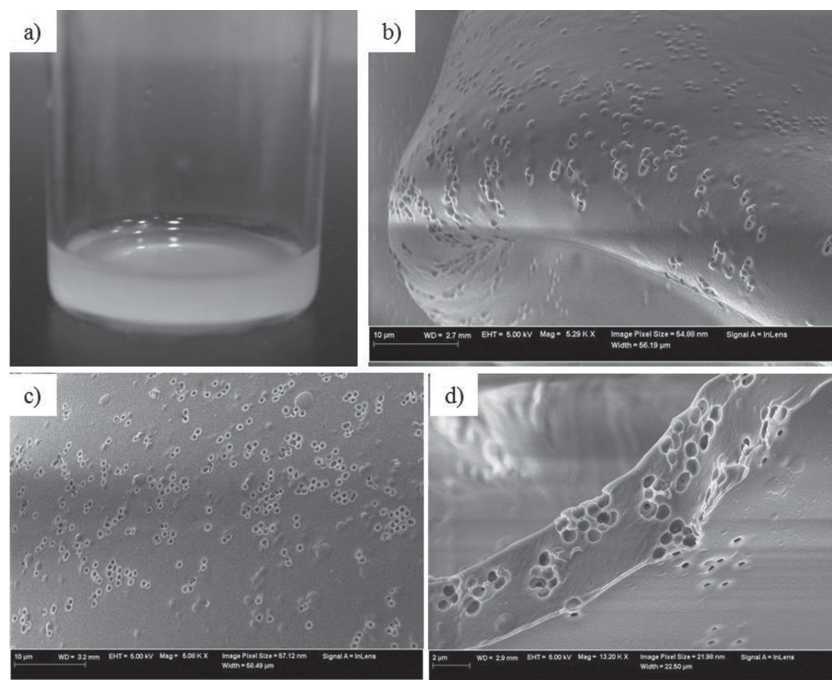


**Figure 5.** a) Photo of vial containing stable colloidal silica suspension; here, the silica is coated with a (heptadecafluoro 1,1,2,2-tetrahydrodecyl) trichlorosilane. SEM images of: b) capsule exterior showing silica particles protruding at the surface, c) capsule exterior after dissolution of the silica template, and d) sectioned particle showing voids throughout the polymeric matrix.

weeks. Osmotic stress-induced bursting can be used as simple release mechanism for these capsules. Additionally, we encapsulate a solution of Nile Red in toluene to investigate the capsules' ability to retain organic dye upon immersion in organic solvents. Through release studies in different organic solvents, we show that both the outer and encapsulated organic phases substantially contribute to increasing the permeability of the PFPE membrane. Controlling the membrane diffusivity through inclusion of an appropriate solvent in the capsule formulation provides a promising approach to tailor the release kinetics. Finally, by incorporating degradable particles we demonstrate the ability to engineer porosity and functionality into an otherwise inert shell material.

The capability of PFPE capsules to retain a diverse set of cargo for an extended period at a high core-shell ratio should make them valuable for controlled release applications that require a low residual footprint of the shell material. Our strategy to synthesize the shell precursor from a PFPE diol allows for future implementation of a variety of specific release mechanisms by incorporation of stimulus-responsive bonds into the polymer matrix.

## 4. Experimental Section

**Materials:** Commercially available chemicals were purchased from reliable sources and used as delivered. PFPE diol ((poly(tetrafluoroethylene oxide-co-difluoromethylene oxide)  $\alpha,\omega$ -diol), 2-isocyanatoethyl methacrylate (IEM), dibutyltin diacetate, Allura Red, and THF were purchased from Sigma-Aldrich Co. (St. Louis, USA). Nile Red was supplied by TCI (Tokyo, Japan). Novec 7100 was obtained from 3M (St. Paul, USA). (Heptadecafluoro 1,1,2,2-tetrahydrodecyl) trichlorosilane was obtained by Gelest, Inc. (Morrisville, USA). The glass microcapillaries were purchased from World Precision Instruments, Inc. (Sarasota, USA). Polyethylene tubing was bought from Scientific Commodities, Inc. (Lake Havasu City, USA). The water used in all reactions was obtained by filtering through a set of millipore cartridges.

**Synthesis of PFPE dimethacrylate:** The perfluoropolyether dimethacrylate was prepared by an adaptation of methods reported previously.<sup>[24–26]</sup> The PFPE diol (10 g, 2.6 mmol,  $M_n = 3800$ ) and IEM (0.82 g, 5.2 mmol) were added in a mixture of Novec 7100 and THF (60:40). A catalytic amount of dibutyltin diacetate (5 mg) was added and the resultant solution was stirred at 50 °C for 24 h under argon atmosphere. Upon completion of the reaction, all volatile compounds were removed under vacuum. An excess of methanol was added to the crude product and the mixture was vortexed and consecutively centrifuged at 3000 rpm for 10 min. After decantation of the supernatant, the PFPE dimethacrylate was dried under vacuum. FTIR spectra were recorded on a Thermo Scientific Nicolet ECO 1000. NMR spectra were obtained at 400 MHz on a Varian Mercury 400 instrument. Quantitative conversion of the hydroxyl groups of the PFPE-diol was determined through comparison of the integrals of the methacrylate moieties and the PFPE backbone.

$^1\text{H}$  NMR (400 MHz,  $\text{CDCl}_3/\text{C}_6\text{F}_6$ ):  $\delta(\text{ppm}) = 2.0$  (s, 6H,  $\text{CH}_3$ ), 3.6 (m, 4H,  $\text{NH}-\text{CH}_2-\text{CH}_2-\text{O}$ ), 4.3 (m, 4H,  $\text{NH}-\text{CH}_2-\text{CH}_2-\text{O}$ ), 4.5 (s, 4H,  $\text{CF}_2-\text{CH}_2$ ), 5.6 (s, 2H,  $\text{O}-\text{C}(\text{CH}_3)\text{CH}_2$ ), 6.1 (s, 2H,  $\text{O}-\text{C}(\text{CH}_3)\text{CH}_2$ ), 6.9 (s, 2H,  $\text{NH}$ ).  $^{19}\text{F}$  NMR (400 MHz,  $\text{CDCl}_3/\text{C}_6\text{F}_6$ ):  $\delta(\text{ppm}) = -55.3$

( $\text{CF}_2\text{O}$ ),  $-78.2/-80.3$  ( $\text{CF}_2-\text{CH}_2$ ),  $-89.2/-91.0$  ( $\text{CF}_2-\text{CF}_2-\text{O}$ ). FTIR:  $\nu = 3348$  and  $2926$  (w, NH),  $1718.1$  (m, CO),  $1637.8$  (w,  $\text{CH}=\text{CH}_2$ ),  $1200-1000\text{ cm}^{-1}$  (s, PFPE chain).

**Microcapsule Fabrication:** The microfluidic devices that were used for the microcapsule fabrication consisted of a glass slide, polyethylene tubing, square glass capillaries, round glass capillaries, and syringe needle tips. The tapered injection capillary was treated with (heptadecafluoro 1,1,2,2-tetrahydrodecyl) trichlorosilane. The tapered collection capillary was coated with the hydrophilic 2-[methoxy(polyethyleneoxy)-propyl]trimethoxysilane. The outer aqueous phase, the middle oil phase, and the inner phase were infused at independently adjustable flow rates using syringe pumps connected to the device by tubing. An aqueous 10 wt% PVA solution was used as the outer aqueous phase and PFPE dimethacrylate containing 0.5 wt% 2,2-dimethoxy-2-phenylacetophenon was used as the middle oil phase. An aqueous solution of 1 wt% Allura Red, an 1.8 M aqueous  $\text{CaCl}_2$  solution, a 0.25 wt% solution of Nile Red in toluene, and an water-in-hexadecane emulsion individually served as inner phase. UV-polymerization of the shell was initiated within the device directly after formation of the template double emulsion droplets using an Omnicure Series 1000 (100 W) UV lamp. The resultant capsules were collected in an aqueous 5 wt% PVA solution. Finally, the PFPE microcapsules were washed with deionized water to remove residual PVA.

**Imaging:** Optical and confocal microscopy images were obtained with a Leica TCS SP5 confocal microscope. Scanning electron microscopy images of the microcapsules were acquired with a Zeiss FESEM Supra55VP or ultrascanning electron microscope using secondary electron detection at 1 kV. Samples were loaded on double-sided carbon tape on an aluminum stud for scanning electron microscopy. UV-vis spectra were recorded with PerkinElmer UV/Vis Spectrometer Lambda 40.

## Acknowledgements

M.A.Z. and N.J.C. contributed equally to this work. This work was supported by the NSF (DMR-1310266), the Harvard Materials Research Science and Engineering Center (DMR-0820484), and the Advanced Energy Consortium (200700518) through the University of Texas, Austin (BEG08-027). Member companies include BP America, Inc., Baker Hughes, Inc., Conoco-Phillips, Halliburton Energy Services, Inc., Marathon Oil Corp., Occidental Oil and Gas, Petrobras, Schlumberger, Shell, and Total.

- [1] C. J. McDonald, M. J. Devon, *Adv. Colloid Interface Sci.* **2002**, *99*, 181.
- [2] G. H. Ma, Z. G. Su, S. Omi, D. Sundberg, J. Stubbs, *J. Colloid Interface Sci.* **2003**, *266*, 282.
- [3] F. Gao, Z. Su, P. Wang, G. Ma, *Langmuir* **2009**, *25*, 3832.
- [4] Y. Zhao, H. C. Shum, L. L. A. Adams, B. Sun, C. Holtze, Z. Gu, D. A. Weitz, *Langmuir* **2011**, *27*, 13988.
- [5] S.-W. Choi, Y. Zhang, Y. Xia, *Adv. Funct. Mater.* **2009**, *19*, 2943.

- [6] B. J. Sun, H. C. Shum, C. Holtze, D. A. Weitz, *ACS Appl. Mater. Interfaces* **2010**, 2, 3411.
- [7] Y. Hennequin, N. Pannacci, C. P. de Torres, G. Tetradis-Meris, S. Chapuliot, E. Bouchaud, P. Tabeling, *Langmuir* **2009**, 25, 7857.
- [8] N. Nihant, C. Grandfils, R. Jérôme, P. Teyssié, *J. Controlled Release* **1995**, 35, 117.
- [9] H. N. Yow, A. F. Routh, *Soft Matter* **2006**, 2, 940.
- [10] H. C. Shum, J. Varnell, D. A. Weitz, *Biomicrofluidics* **2012**, 6, 12808.
- [11] M. P. Krafft, J. G. Riess, *Biochimie* **1998**, 80, 489.
- [12] J. G. Riess, M. P. Krafft, *MRS Bull.* **1999**, 24, 42.
- [13] W. R. Jones, T. R. Bierschenk, T. J. Juhlke, H. Kawa, R. J. Lagow, *Ind. Eng. Chem. Res.* **1988**, 27, 1497.
- [14] A. Vitale, M. Quaglio, M. Cocuzza, C. F. Pirri, R. Bongiovanni, *Eur. Polym. J.* **2012**, 48, 1118.
- [15] A. S. Utada, L. Chu, D. R. Link, C. Holtze, D. A. Weitz, *MRS Bull.* **2007**, 32, 702.
- [16] N. Vilanova, C. Rodríguez-Abreu, A. Fernández-Nieves, C. Solans, *ACS Appl. Mater. Interfaces* **2013**, 5, 5247.
- [17] J. Guery, J. Baudry, D. A. Weitz, P. M. Chaikin, J. Bibette, *Phys. Rev. E* **2009**, 79, 060402.
- [18] S. S. Datta, S.-H. Kim, J. Paulose, A. Abbaspourrad, D. R. Nelson, D. A. Weitz, *Phys. Rev. Lett.* **2012**, 109, 134302.
- [19] A. Abbaspourrad, W. J. Duncanson, N. Lebedeva, S.-H. Kim, A. P. Zhushma, S. S. Datta, P. A. Dayton, S. S. Sheiko, M. Rubinstein, D. A. Weitz, *Langmuir* **2013**, 29, 12352.
- [20] H. Chaouk, J. S. Wilkie, G. F. Meijs, H. Y. Cheng, *J. Appl. Polym. Sci.* **2001**, 80, 1756.
- [21] A. Griset, J. Walpole, R. Liu, *J. Am. Chem. Soc.* **2009**, 131, 2469.
- [22] S.-H. Kim, A. Abbaspourrad, D. A. Weitz, *J. Am. Chem. Soc.* **2011**, 133, 5516.
- [23] W. Wang, M.-J. Zhang, R. Xie, X.-J. Ju, C. Yang, C.-L. Mou, D. A. Weitz, L.-Y. Chu, *Angew. Chem. Int. Ed. Engl.* **2013**, 52, 8084.
- [24] A. Priola, R. Bongiovanni, G. Malucelli, *Macromol. Chem. Phys.* **1997**, 198, 1893.
- [25] R. Bongiovanni, A. Medici, A. Zompatori, S. Garavaglia, C. Tonelli, *Polym. Int.* **2012**, 61, 65.
- [26] J. P. Rolland, R. M. Van Dam, D. A. Schorzman, S. R. Quake, J. M. DeSimone, *J. Am. Chem. Soc.* **2004**, 126, 2322.

Received: October 27, 2014

Revised: December 2, 2014

Published online: